Tellus (1995), 47B, 535–549
Printed in Belgium – all rights reserved

TELLUS
ISSN 0280–6509

Measurements of carbon dioxide on a very tall tower

By PETER S. BAKWIN* and PIETER P. TANS, *Climate Monitoring and Diagnostics Laboratory, National Oceanic and Atmospheric Administration, Boulder, Colorado, 80303, USA*, CONGLONG ZHAO, *Cooperative Institute for Research in Environmental Science, University of Colorado, Boulder, Colorado, 80309, USA*, WILLIAM USSLER, III, *Marine Sciences Curriculum, University of North Carolina, Chapel Hill, North Carolina, 27599, USA* and EVERETT QUESNELL, *Atmospheric Research and Exposure Assessment Laboratory, United States Environmental Protection Agency, Research Triangle Park, North Carolina, 27711, USA*

(Manuscript received 26 September 1994; in final form 10 February 1995)

ABSTRACT

We present a continuous, 2-year long record of carbon dioxide (CO_2) mixing ratio at three altitudes up to 496 m above the ground on a television transmitter tower in the southeastern United States. The data show strong diurnal and seasonal variations, and large vertical gradients. The diurnal cycles are modulated by surface uptake and release by vegetation and soils, emissions from fossil fuel combustion, and by the diurnal development of the planetary boundary layer. Gradients of 1–2 ppm between 496 m and 51 m are typically observed during summertime afternoons, due to vigorous photosynthetic uptake. With increasing altitude the magnitude of the diurnal cycle is damped, and daily average mixing ratios decrease, caused by coincident changes in the sign and magnitude of the surface flux, and changes in vertical stability of the boundary layer over the course of the day. Measurements at 496 m give an approximate measure (within a few tenths of a ppm) of the afternoon mean mixing ratio in the convective boundary layer. Vertical gradients between 51 m and 496 m are typically close to zero, and monthly mean mixing ratios increase slowly between November and April, indicating that biological activity is minimal during this period. The amplitude of the seasonal cycle of CO_2 is larger at the tower site than at marine boundary layer and mountaintop sites which are at nearly the same latitude, because of the proximity of the tower site to terrestrial sources and sinks. Comparison of our continental tower data with data from "background" sites should provide a strong constraint for regional and global models of terrestrial CO_2 fluxes. We also present data from weekly flask samples taken from the 496 m level and which have been analyzed for methane (CH_4), carbon monoxide (CO), and the stable isotopes of carbon in CO_2 ($\delta^{13}C$). The flask data provide further information about the processes that drive observed changes in CO_2 mixing ratio at the tower.

1. Introduction

The atmospheric burden of CO_2 has been monitored at many sites world-wide for up to 35 years (Keeling et al., 1989; Conway et al., 1988, 1994). These measurements have shown that CO_2 increased steadily during the past few decades at a rate approximately equal to 60% of the annual input from fossil fuel burning (Keeling et al., 1989). However, significant inter-annual changes in the global growth rate for CO_2 have frequently occurred (Keeling et al., 1989; Conway et al., 1994). The largest anomaly in the CO_2 growth rate that has been observed occurred during 1992, when the global growth rate was only about 20% of the fossil fuel input, and the growth rate for the entire Northern Hemisphere was near zero (Conway et al., 1994).

Analysis of the latitudinal variation in atmospheric CO_2, along with known source strengths

* Corresponding author.

from industrial activity, has led to the conclusion that a large sink for CO_2 exists at temperate to high latitudes in the Northern Hemisphere (Tans et al., 1990; Conway et al., 1994). Further, recent measurements of the stable isotopic composition of CO_2 ($\delta^{13}C$) from a globally distributed network of sampling stations have identified the terrestrial biosphere of the northern midlatitudes as a major component of this "missing sink", at least for 1992 (Ciais et al., 1995). However, current sampling networks for CO_2 and $\delta^{13}C$ are heavily weighted toward the marine boundary layer, and terrestrial systems are greatly under-represented (Tans, 1991). This is because CO_2 mixing ratios are much less variable in marine areas than over the continents, so that accurate monthly and annual mean mixing ratios can be obtained by weekly flask sampling, allowing a large number of stations to be sampled regularly.

Tans (1991) proposed a strategy to determine CO_2 mixing ratios representative of continental areas, and thereby allow terrestrial net fluxes to be better quantified using global models. The methods proposed by Tans (1991) were designed to minimize the effects of local sources and sinks on mixing ratio measurements to allow regionally representative means to be determined. One component of this strategy was continuous monitoring of CO_2 (and other trace gas species) on existing very tall towers. Here we report the first two years of CO_2 measurements taken on a very tall tower (610 m height) in the southeastern United States.

2. Experimental

2.1. Study site

In June 1992, we began continuous measurements of CO_2 on a 610 m tall television and FM radio transmitter tower in a rural area of eastern North Carolina (35.37° N, 77.39° W, 9 m above sea level). Use of the tower and space in the transmitter building for our analytical and data acquisition equipment have been provided by American Family Broadcasting, Inc.

The area surrounding the tower is mixed agricultural and forest, with some light industry. Forests comprise approximately 47% of the surrounding three county region (Pitt, Lenoir, and Greene counties), agricultural crops and pasture 42%, and developed lands 11% (Sheffield and Knight, 1986; US Department of Commerce, 1989). The mix of surface cover types is patchy on scales of a few hundred to a few thousand meters. The most common crops are corn (13.8% total land area), soybeans (11.5%), tobacco (3.3%), wheat (2.2%), and peanuts (0.6%) (US Department of Commerce, 1989). Forests are mixed hardwoods (63% area, oak-gum-cypress forests dominant) and conifers (37% area, *Pinus taeda* is dominant), often with a dense understory. Forest canopy heights are typically 20–30 m. Relief is minimal, soils are often very poorly drained, and forested wetlands are common along major tributaries. Upland soils are typically sandy clay loams developed on Tertiary and Cretaceous marine sediments (Karnowski et al., 1974). The region around the tower appears typical of a large area including eastern North and South Carolina, and much of eastern Virginia and Georgia.

2.2. Carbon dioxide analysis

Tubes for trace gas sampling (1 cm inner diameter, DuPont Dekabon type 1300) were mounted on the tower with inlets at 51, 123, and 496 m height above the ground. Air was continuously drawn through each of the tubes at a flow rate of about 4 L min^{-1} using diaphragm pumps located in the transmitter building (Fig. 1). The sample air from each level was pressurized to about 0.7 bar above ambient pressure and was then passed through a glass trap for liquid water maintained at ≈ 4°C. The traps were continuously purged of water to minimize loss of CO_2 to the liquid phase. From each dried sample stream a flow of 100 cm^3 min^{-1} was diverted through a 16-position sampling valve (Valco Instruments, Houston, Texas), which was used to select between sample and calibration gas. The common port of each valve was connected to a mass flow controller (Tylan General, Torrence, California), which maintained a constant flow through a CO_2 analyzer. Before analysis, this air was further dried to a dew point of −25°C (as determined by measurements in the laboratory prior to field deployment) using a Nafion drier (Permapure, Toms River, New Jersey, model MD-250-72P Mini Drier), so that the water vapor interference and dilution effects were <0.1 ppm (parts per million by mole fraction) equivalent CO_2. Analysis for CO_2 mole fraction was carried out by IR absorption spectroscopy using Li-Cor (Lincoln,

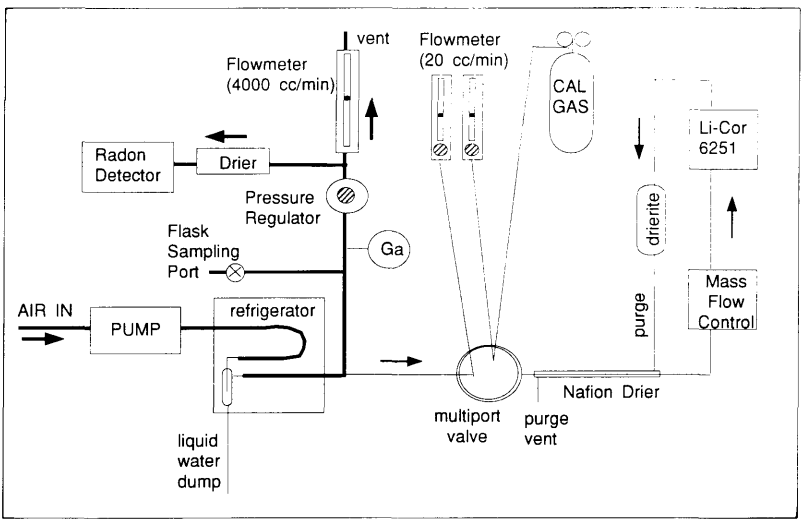

Fig. 1. Apparatus for the measurement of carbon dioxide. Three sets of equipment were used to carry out measurements at 51, 123, and 496 m on a television transmitter tower eastern North Carolina.

Nebraska) model 6251 analyzers. The reference cell of each analyzer was flushed at a flow rate of 10 cm^3 min^{-1} with a compressed gas standard containing $\approx$330 ppm CO_2 in air.

The Li-Cor analyzers exhibit non-linear response which can be well approximated over the range of interest using a second order polynomial. We calibrated the instruments with four standards spanning the range 330–420 ppm. Each standard was analyzed for 2 min during each calibration sequence, and calibrations were carried out every 3 h. The root mean squares of the residuals from the 4-point fits were generally less than 0.1 ppm. The reference and sample cells were not pressure controlled and the instrument span was dependent on ambient pressure, as expected. Each Li-Cor was "zeroed" every 36 min using the 330 ppm standard, in order to account for short-term drift in the instrument zero, which varied somewhat with temperature. Linear interpolation of the data between each "zero" and calibration was used.

Standard and reference gas cylinders were filled with ambient air at Niwot Ridge, Colorado. The air was dried using magnesium perchlorate and either scrubbed with Ascarite or spiked using a 10% CO_2-in-air mixture to obtain mixing ratios below or above ambient levels, respectively. The cylinders were referenced to CMDL primary standards (which are tied to the WMO X85 mole fraction scale, Thoning et al., 1987) before use, and were referenced to 4 "station" standards at the site once each month. The "station" standards have a long lifetime (years) and provide a long-term basis of comparison for the working standards. Working standard mixing ratios determined by comparison to station standards were within 0.2 ppm of those determined by calibration at CMDL, except for standards outside of the range of the current CMDL reference scale (310–395 ppm), which differed by as much as 0.5 ppm.

Sampling and calibration sequences were controlled and data were read and pre-processed using a PC running under the multi-tasking operating system QNX (QNX Software Systems, Kanata, Ontario, Canada). 30-min averages of the ambient data and 30 s averages of the calibration data were computed and transmitted to Boulder each day via modem.

2.3. *Supporting measurements*

Sensors for wind speed and direction, temperature and humidity were placed at the same three levels (51, 123, and 496 m) as the tubes for CO_2 sampling, but subsequently the upper sensors were moved to 404 m height because of electromagnetic interference from the television and FM radio transmitters located near the top of the tower. Data from the top level sensors were

Tellus B/47/5-2

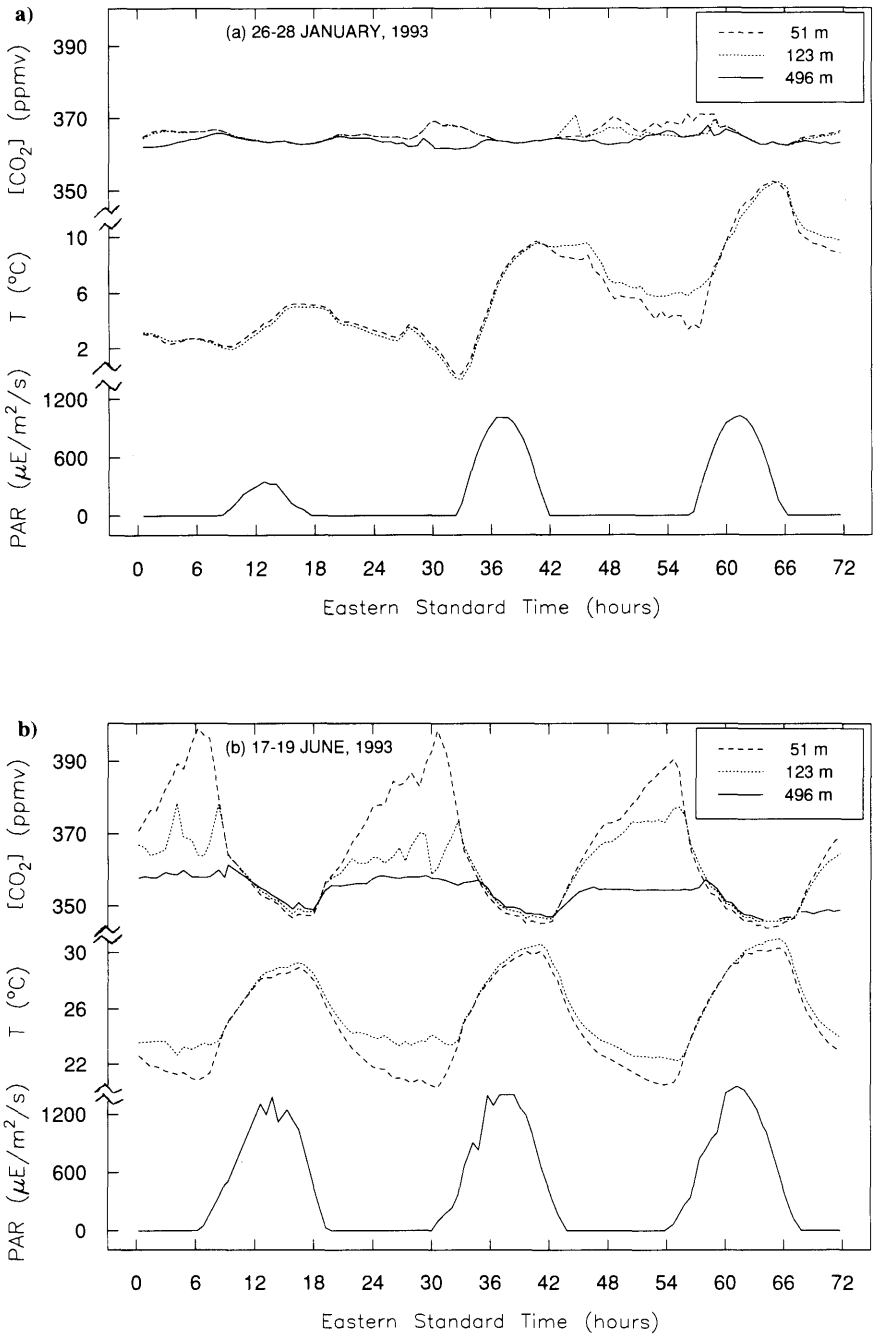

Fig. 2. Three days of CO_2, temperature, and photosynthetically active radiation (PAR) data in (a) January, and (b) June, 1993. Temperature data from the top level were not available because of instrument problems.

collected by a remote computer located on the tower, and were transmitted to the main data acquisition computer via a wireless (915 MHz) modem (Proxim, Mountain View, California). Analog data from the lower levels (51 and 123 m) were transmitted over cables using current loops. Ambient pressure at the surface was measured using an analog barometer (A.I.R., Inc., Boulder, Colorado). Incident photosynthetically active radiation (PAR) was measured using a Li-Cor model 190S quantum sensor. Soil temperatures were measured at 10 cm depth at 15 locations in a field adjacent to the tower and in the margin of a forest nearby, but a lightning strike in October, 1993, destroyed 13 of those sensors.

Concentrations of radon-222 were measured at 0.5, 51, 123, and 496 m, and will be reported in detail in a future paper (Ussler, W., III, Martens, C.S. and Bakwin, P.S., *Quantifying boundary layer exchange of trace gases using measurements of Rn-222 on a tall tower*, manuscript in preparation). Radon-222 originates in the soil from radioactive decay of radium-226 and has a half-life of 3.8 days, making it an excellent tracer for soil/atmosphere gas exchange and continental air masses.

Paired flask samples (2.5 L) were collected weekly from the 496 m level for analysis for CH_4, CO_2, CO, and $\delta^{13}C$ and $\delta^{18}O$ in CO_2, following standard CMDL procedures (Steele et al., 1987; Conway et al., 1988; Novelli et al., 1992; Trolier, M., White, J. W. C., Tans, P. P., Masarie, K. A. and Conway, T. J., *Monitoring the isotopic composition of atmospheric CO_2: measurements from the NOAA/CMDL global air sampling network*, manuscript in preparation). The CO_2 data from the flask samples provide a further validation of the on-site calibrations. The mean difference between flask and continuous CO_2 measurements was not significantly different from zero, however, due to mismatched timing between the flask samples and averaging of continuous data, and to the high degree of variability of ambient CO_2, the r.m.s. of residuals from a one-to-one relationship was 3–4 ppm.

3. Results and discussion

3.1. Diurnal and seasonal cycles

Fig. 2 shows the time series of CO_2 and temperature at each height, and incident PAR, for 3

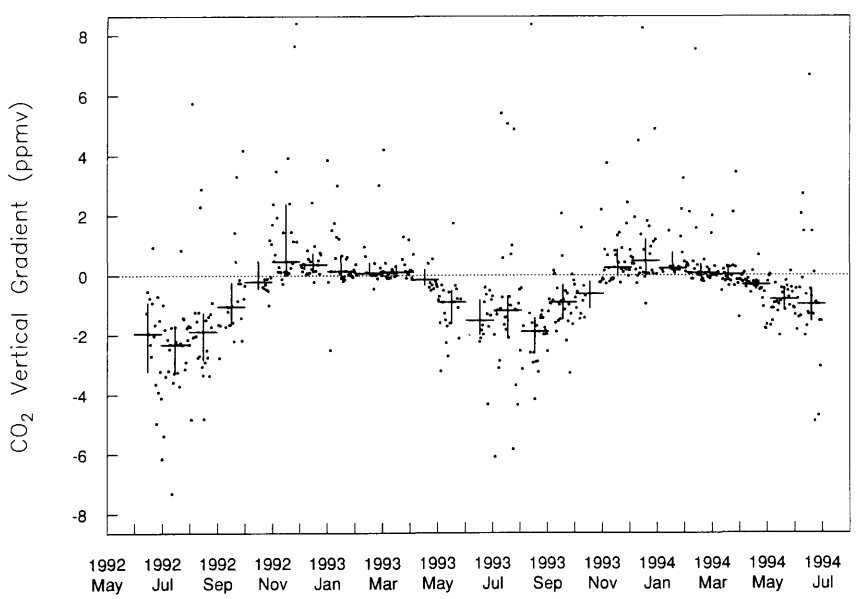

Fig. 3. Gradients of CO_2 mixing ratio between 51 and 496 m above the surface in the afternoon (1500–1700 EST) for each day of observations. 8 points with gradients in the range 9 to 25 ppm, and 2 points with gradients in the range −12 to −9 ppm are not shown. The large crosses denote monthly medians (horizontal bars) and inner quartiles (vertical bars) of the data.

consecutive days in January and June, 1993. In the afternoon in summer the CO_2 gradient is positive upwards, with a magnitude of typically about 1–3 ppm between 51 and 496 m (see Fig. 3), due to vigorous photosynthetic uptake of CO_2 at the surface. At night a shallow inversion forms, and mixing ratios near the ground increase rapidly as a result of plant and soil respiration and emissions from fossil fuel combustion, often reaching in excess of 400 ppm at 51 m. The diurnal cycle is damped at higher altitudes; the amplitude is typically 7–10 ppm at 496 m in summer. A morning pulse of CO_2 is often observed at 123 and 496 m as CO_2 stored in the nocturnal stable layer is mixed upward with the onset of convection. The nocturnal accumulation of CO_2 at low altitudes is reflected in 10–15 ppm higher daily mean mixing ratios at 51 m than at 496 m in summer (Table 1).

In winter the biologically driven surface sources and sinks are much smaller, and the diurnal variation at all altitudes is greatly reduced. Between early November and mid-April the afternoon gradient is typically close to zero (<0.5 ppm, Fig. 3), except when strong daytime inversions occur, and surface emissions lead to large mixing ratios near the ground, and gradients of several ppm between 51 and 496 m (Fig. 3).

To estimate the relative importance of biological fluxes compared to fossil fuel sources we compute the area-averaged fossil fuel emissions of CO_2 from all of North Carolina (1.27×10^7 ha, population 6.4×10^6 in 1990), assuming that the per-capita use of fossil fuels by residents of North Carolina is equal to the average for the North America (5280 kgC in 1990, Marland et al., 1994). We find a mean fossil fuel flux to the atmosphere of 0.3 kgC ha^{-1} h^{-1}, similar to the wintertime respiration flux measured at Harvard Forest,

Table 1. *Monthly statistics for daily mean CO_2 mixing ratios (ppm)*

		Mean	Median	Mean	Median	Mean	SD	Median	LQ	UQ	N
Year	Month	51 m		123 m		496 m					
1992	6	362.85	363.95	NA	NA	352.49	3.22	352.80	349.78	355.13	14
	7	368.17	370.19	NA	NA	353.86	4.42	353.96	351.22	356.84	25
	8	364.58	365.82	357.52	358.90	349.96	6.51	350.58	343.52	354.38	23
	9	363.52	362.74	NA	NA	349.83	4.44	351.10	346.47	352.54	18
	10	366.19	365.35	NA	NA	356.29	5.19	354.99	352.31	359.71	30
	11	369.14	367.74	365.86	364.47	361.40	4.32	360.45	358.11	363.29	29
	12	367.20	366.81	366.24	365.52	361.88	3.12	361.33	359.80	363.66	29
1993	1	369.08	366.66	368.18	366.23	364.06	3.78	363.21	361.60	366.03	28
	2	366.65	365.87	366.05	365.21	364.56	2.89	364.08	362.53	364.64	13
	3	369.35	368.76	368.00	366.85	365.71	3.48	364.88	362.90	368.64	23
	4	367.39	367.47	366.71	366.46	364.00	2.64	363.58	362.50	365.19	23
	5	367.16	366.37	362.77	362.54	358.68	3.10	359.08	355.68	361.34	23
	6	NA	NA	361.87	361.67	355.35	2.84	355.48	353.46	357.82	22
	7	370.11	369.16	361.52	361.47	353.80	3.80	353.85	351.10	356.46	31
	8	364.45	364.35	355.90	354.98	350.76	4.38	351.80	347.24	354.56	26
	9	370.20	366.24	363.07	361.92	355.83	4.45	354.88	353.50	358.46	29
	10	365.79	363.09	362.15	360.94	356.96	4.83	355.81	353.74	359.00	11
	11	368.83	368.52	366.59	364.81	362.22	3.78	362.29	359.20	364.59	27
	12	369.59	369.73	368.00	367.99	364.83	2.77	364.99	362.43	367.18	29
1994	1	369.89	369.68	368.94	368.12	365.99	3.23	365.49	364.42	367.19	20
	2	370.80	369.46	369.07	367.27	366.23	4.32	364.89	363.21	367.43	28
	3	368.80	369.83	367.17	366.90	365.15	2.15	364.77	363.77	366.14	25
	4	369.71	368.83	367.05	366.51	363.42	2.49	363.74	361.67	364.99	29
	5	366.28	366.35	363.49	363.38	360.63	2.94	360.99	359.47	362.02	26
	6	368.62	368.07	364.02	363.48	358.48	2.66	358.24	356.94	359.34	29

LQ and UQ denote lower and upper quartiles, respectively, NA indicates data not available.

Massachusetts (Wofsy et al., 1993). Assuming an impenetrable inversion at 200 m above the ground this flux would cause CO_2 to increase at a rate of about 0.3 ppm h^{-1} below the inversion. These conditions, persisting for a full day, could account for the large afternoon gradients in wintertime (Fig. 3). It is of note that the largest (>5 ppm) wintertime gradients typically develop over 2–4 days. However, this rate of increase is small compared to the nightly increase in CO_2 at 51 and 123 m in summer (Fig. 2b). Biological activity clearly dominates the CO_2 source from fossil fuel combustion at this rural site in summer.

To obtain monthly statistics of the data we first computed daily average CO_2 mixing ratios for each height by interpolating the observations linearly in time so that each hour is represented. Days with data gaps of longer than 2.5 h were excluded, and 85% of the days between 14 June 1992, and 30 June 1994, are represented in the data set for 496 m. The results are presented in Table 1, and statistics of the daily afternoon mixing ratios (1500–1700 EST) at 496 m are presented in Table 2. In general, daily means are 0–5 ppm higher than afternoon mixing ratios, with the largest differences in summer. Minimum CO_2 values were observed during August, followed by a rapid increase through the fall. During winter CO_2 mixing ratios increased more slowly, and peak values were observed in February or March. The amplitude of the seasonal cycle was about 15 ppm.

Table 2. *Monthly statistics for afternoon (1500–1700 EST) mean CO_2 mixing ratios at 496 m height*

Year	Month	Mean	SD	Median	LQ	UQ	N
1992	6	347.07	3.78	346.90	343.86	349.28	17
	7	349.96	6.07	350.67	345.03	354.90	30
	8	345.04	8.00	342.15	338.96	352.42	27
	9	347.40	4.39	348.14	344.72	350.39	23
	10	355.36	6.57	353.79	350.34	360.65	31
	11	360.28	4.49	360.08	356.21	363.94	26
	12	361.89	3.79	361.19	359.77	362.68	30
1993	1	364.17	4.44	363.02	361.16	366.26	29
	2	363.83	3.13	363.35	360.85	364.67	19
	3	365.51	4.45	364.76	361.89	367.58	24
	4	362.45	2.87	362.31	360.15	364.41	29
	5	355.92	4.47	357.09	352.37	359.71	29
	6	351.88	3.25	350.95	349.83	355.01	26
	7	350.40	5.05	350.48	347.55	354.90	31
	8	347.82	4.54	347.75	345.15	351.27	25
	9	354.67	5.30	353.86	351.69	357.06	30
	10	356.51	7.04	354.22	351.74	358.69	13
	11	362.43	5.39	360.61	359.11	364.91	29
	12	365.15	3.97	364.74	363.06	366.87	30
1994	1	366.22	3.72	365.55	363.82	368.05	22
	2	365.82	4.76	364.23	362.59	366.98	28
	3	364.43	2.62	363.97	363.13	365.40	28
	4	362.26	3.09	361.98	360.03	364.43	30
	5	358.10	3.22	358.21	354.95	360.44	29
	6	354.84	3.20	354.63	352.22	356.70	30

LQ and UQ denote lower and upper quartiles, respectively.

Periods of strong stable stratification may disproportionately influence our results, since surface fluxes may lead to unusually large vertical gradients during those periods. To check this possibility, we computed statistics of CO_2 mixing ratios for only those hourly intervals when the wind speed at 51 m exceeded 3 m/s, which should exclude periods of strong stratification. However, the results did not differ greatly from those presented in Tables 1, 2. Further, during some periods large amounts of data were excluded using this criterion. For example, for morning periods (0600–1200 EST) in July only about 15% of the data were retained. The use of medians, rather than means, in Figures 3 and 6 (see below) should minimize the effect of strong stratification on the statistical presentation of the results.

Mixing ratios at 496 m for the last 6 months of 1993 and the first 6 months of 1994 were about 1.6 ppm higher on average than for the same period of 1992–1993 (Table 1), although with fairly large variability (relative standard deviation for the difference in monthly medians = 0.86). This increase is somewhat larger than the growth at Mauna Loa Observatory (MLO) of about 0.9 ppm for the same period (T. Conway, personal communication, 1994), but is similar to the annual average global rate of increase of CO_2 for 1981–1989 (1.5 ppm yr^{-1}, Conway et al., 1994). The global growth of CO_2 mixing ratios was suppressed during 1992, most likely associated with a climate perturbation (cooling) due to the eruption of Mt. Pinatubo in July, 1991 (Conway et al., 1994). Global mean temperatures began to recover in the latter half of 1993 (Climate Analysis Center, 1994), and temperatures at the National Climatic Data Center surface station at Newbern, NC (50 km SE of our site), were 0.6°C warmer, on

average, during the second half of 1993 and first half of 1994 than for the same period in 1992–1993. If a change in the balance of continental sources and sinks were responsible for the slow growth of CO_2 in the atmosphere during 1992 then CO_2 growth rates at continental locations might be expected to lead more remote sites as temperatures recovered from perturbed conditions. Our results are consistent with this scenario.

3.2. *Mixing ratio profiles in the convective boundary layer*

In this section we examine the degree to which the CO_2 measurements on the tower are representative of the entire planetary boundary layer. It is evident from Fig. 2 that surface fluxes and vertical mixing have a strong influence on the mixing ratios of CO_2, even 496 m above the ground. A theoretical framework to relate mixing ratio profiles to surface and entrainment fluxes has been developed and tested against observational data for the convective boundary layer (CBL), so we focus on this case. We compute the vertical profile of CO_2 mixing ratio from a range of likely values of the surface (F_0) and entrainment (F_{z_i}) fluxes, CBL height (z_i), and convective velocity scale (w_*, which is proportional to the cube root of the surface heat flux), using flux-gradient relationships for the CBL (Wyngaard and Brost, 1984, their equation 18),

$$\frac{\partial CO_2}{\partial z} = -g_b \frac{F_0}{z_i w_*} - g_t \frac{F_{z_i}}{z_i w_*}, \qquad (1)$$

where z is the vertical coordinate, and g_b and g_t are gradient functions for bottom-up (driven by surface buoyancy production) and top-down (driven by entrainment) mixing, respectively. The gradient functions are simple functions of z/z_i, and have been determined from large-eddy simulations by Moeng and Wyngaard (1984, 1989), which have been verified to a limited extent by Davis (1992) using aircraft and tethered balloon data.

During the mid-afternoon (1500–1700 EST) CO_2 mixing ratios at our measurement heights generally did not change rapidly (e.g., Fig. 2b); evidently the surface and entrainment fluxes were roughly equal during this period. Surface fluxes in the range -0.3 to -0.8 ppm m s^{-1} (-5 to -14 kgC ha^{-1} h^{-1}, where negative fluxes are downward) are generally consistent with the measured afternoon vertical gradients in summer, and with CO_2 fluxes measured above an oak-hickory forest in Tennessee (Baldocchi et al., 1987). In the morning (in summer) a pulse of CO_2 that was stored under the nocturnal inversion was typically observed at 123 m around 0800 EST, and at 496 m about 2 hours later (Fig. 2b), indicating that z_i grew at roughly 5 cm s^{-1} during this period. If CBL growth continued at this rate until 1600 EST then a CBL depth of about 1600 m would be reached. Examination of temperature profiles from rawinsondes launched at 0000 UT (1900 EST) from the Raleigh-Durham Airport (140 km NW of our site) confirm that afternoon CBL depths were typically around 1600 m in summer. Therefore, we computed mixing ratio profiles for z_i in the range 1200–2000 m. Typical values of w_* for the afternoon CBL are 1.5–2.0 m s^{-1} (Stull, 1988). Since the gradient functions are not expected to be accurate near the surface and CBL top (Wyngaard and Brost, 1984), we computed the mean CO_2 mixing ratio for altitudes between $0.1z_i$ and $0.8z_i$.

Fig. 4 shows some example profiles of CO_2 through the CBL predicted from eq. (1) with $z_i =$ 1600 m. Measured afternoon median mixing ratios

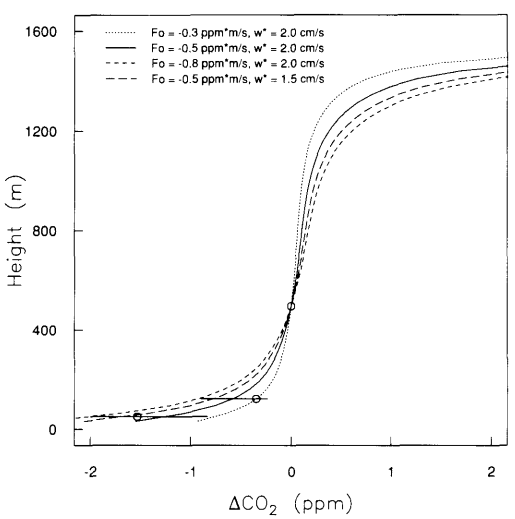

Fig. 4. Vertical profile of CO_2 (difference from 496 m height) predicted for the convective boundary layer using eq. (1), with $z_i = 1600$ m, and other conditions as indicated. The points show medians, and the horizontal bars show the range of the lower and upper quartiles, of the afternoon (1500–1700 EST) observations taken during June 1993.

for June 1993, are plotted for comparison. For the range of conditions indicated above, the CBL mean mixing ratio differs from the mixing ratio at 496 m by 0.0–0.3 ppm, with the largest difference for large z_i, large uptake flux, and small w_*. We find that the mixing ratio at 496 m approximates the mean for the summertime afternoon CBL, within a few tenths of a ppm. In other seasons fluxes are generally smaller, and boundary layer depths are shallower, so it is likely that this result is true for the full year. The CO_2 profiles predicted by eq. (1) are generally consistent with the measurements for CO_2 fluxes in the range -0.3 to -0.8 ppm m s^{-1}. Large deviations from the predicted profiles occur when conditions are not convective.

3.3. *Comparison with background sites*

Fig. 5 shows a comparison of CO_2 data from mid-latitude Northern Hemisphere background sites of the CMDL flask sampling network (Conway et al., 1994): Mauna Loa, Hawaii (MLO, 19.53°N, 155.58°W, 3400 m above sea level), Bermuda (two sampling sites near sea level on the island: BME, 32.37°N, 64.65°W, and BMW, 32.27°N, 65.88°W, we refer to the Bermuda sites together as BMX), and Niwot Ridge, Colorado (NWR, 40.05°N, 105.63°W, 3750 m above sea level). The data from individual flask pairs from each site have been smoothed in time using the methods of Thoning et al. (1989). To identify data representative of "background" conditions, residuals from the smooth curve were computed and points farther than 2 residual standard deviations (σ) from the curve were eliminated, and the remaining points refitted with a smooth curve. A similar procedure was used by Conway et al. (1988, 1994), but they removed data points farther than 3σ from the initial curve. The resulting smooth curves for all three sites in Fig. 5 with filtering at 2σ and 3σ are very similar except that the minimum in 1992 at BMX is about 2.5 ppm lower with removal of only points farther than 3σ from the initial smooth curve.

The timing of the seasonal cycles at NWR and BMX is very similar, and lead MLO by a few weeks. The wintertime maxima at NWR and BMX are very similar in all years, as are the summertime minima in 1989, 1990, and 1993. However, in 1991 and 1992 the summertime minima at BMX were

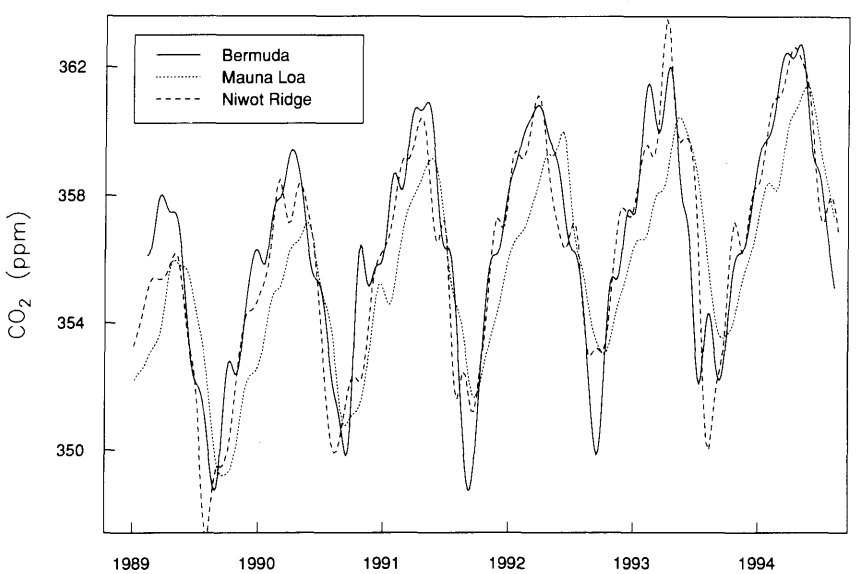

Fig. 5. Smoothed CO_2 mixing ratios from four "background" sites of the CMDL flask sampling network (see text). The flask data were fit with a smooth curve (Thoning et al., 1989) and residuals were computed. Data points lying farther than 2 residual standard deviations from the curve were eliminated, and the remaining points were refitted with a smooth curve.

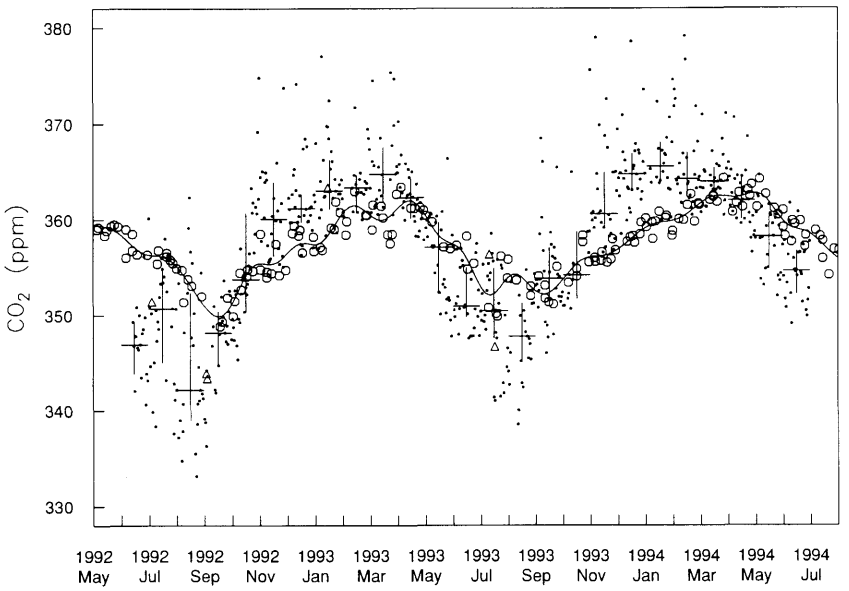

Fig. 6. Daily afternoon (1500–1700 EST) CO_2 mixing ratios at 496 m on the North Carolina tower (points) and CMDL flask data from Bermuda (open symbols). The large crosses denote monthly medians (horizontal bars) and inner quartiles (vertical bars) of the tower data, and the solid line is a fit to the Bermuda data (circles), with points lying more than 2 residual standard deviations from the curve plotted as triangles.

substantially (about 4 ppm) lower than at NWR. Low summertime CO_2 mixing ratios at Bermuda are typically observed during events of transport of air from the North American continent. For example, air samples taken at BME and BMW on September 3 and 4, 1992, respectively (plotted as triangles in Fig. 6), show values 5–10 ppm below those obtained for the previous and subsequent weeks. These low values fall within the range of afternoon mixing ratios observed during the same period at the tower (Fig. 6), suggesting that the samples may reflect transport of low-CO_2 air from the continental boundary layer to Bermuda. Isobaric back trajectory analysis (J. Harriss, personal communication, 1993) shows rapid (1–2 day) transport of air from the southeast United States to Bermuda during this period. Such events may have been more common in 1991 and 1992 than in other years, or may simply have been more heavily represented in the twice-weekly flask samples for those years. The seasonal amplitude at MLO is typically 1–3 ppm smaller than at NWR. The phase and amplitude of the seasonal cycle of CO_2 in the Northern Hemisphere is controlled largely by biological processes on land (Fung et al., 1987), so the phase shift and somewhat lower amplitude at MLO likely reflects the isolation of the site from continental boundary layer air.

From the overall similarity in the timing and amplitudes of the seasonal cycles at BMX and NWR we conclude that the composition of air collected at these sites is generally representative of the free troposphere over North America at 30–40° N. However, during some summer periods CO_2 mixing ratios at BMX are strongly influenced by sources and sinks on the North American continent.

In Fig. 6 the daily afternoon (1500–1700 EST) mean CO_2 mixing ratios at 496 m height on the North Carolina tower are plotted with the flask data from BMX. We have argued that the afternoon values at the tower are generally close to the afternoon means for the whole CBL, and that the mixing ratios at BMX typically reflect free tropospheric values. Hence, the difference between the mixing ratios at these two locations gives a measure of the afternoon drawdown or increase in

CO_2 within the CBL at the tower site due to regional surface fluxes.

In winter the afternoon means at 496 m on the tower are generally 2–5 ppm higher than at BMX, likely reflecting net respiration and CO_2 emissions from fossil fuel combustion around the tower site. In summer afternoon means at the tower are typically 2–10 ppm lower than at BMX, indicating rapid daytime photosynthesis in the vicinity of the tower. This information should be useful to constrain regional and global models of CO_2 exchange on the North American continent.

3.4. *Isotopic composition of CO_2 ($\delta^{13}C$)*

The isotopic composition of CO_2 in flask samples collected weekly at 496 m height is shown in Fig. 7, plotted against the reciprocal of CO_2 mixing ratio. In this plot the intercept ($1/CO_2 = 0$) gives a measure of the isotopic composition of the CO_2 source or sink that causes the observed variations in CO_2 abundance (Keeling, 1961). Winter (November–April) and summer (May–October) data show significantly different slopes and intercepts. In winter the CO_2 source has an isotopic

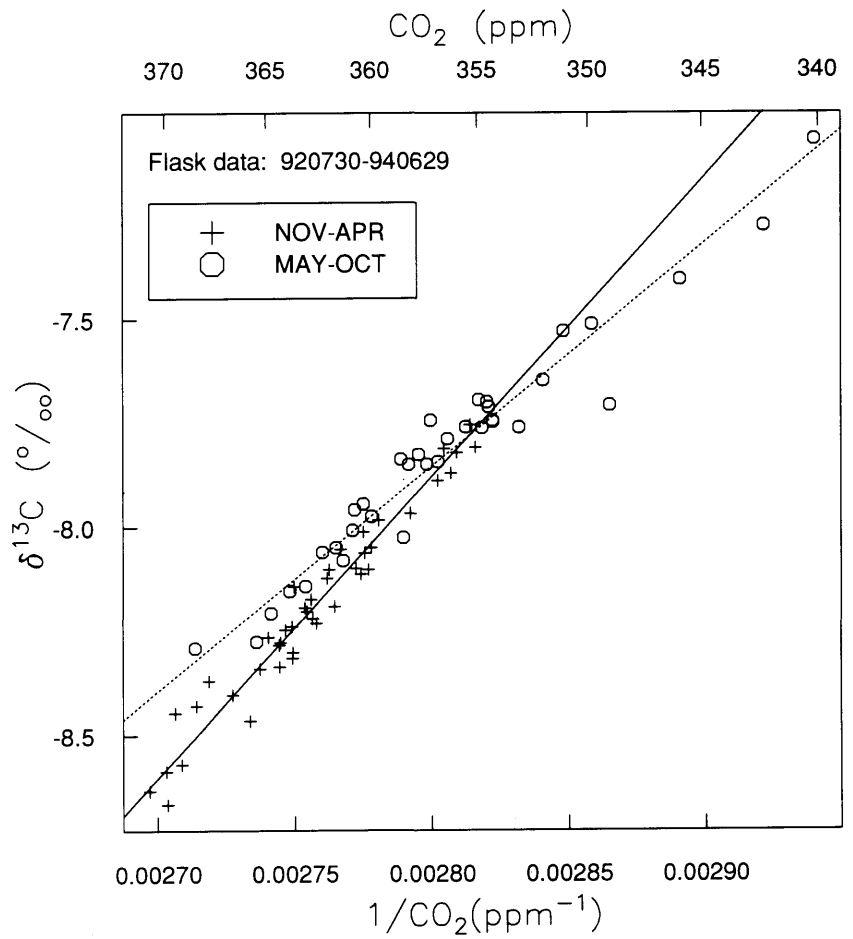

Fig. 7. The relationship between $\delta^{13}C$ and CO_2 in flask samples from 496 m. Winter (November–April, plusses) and summer (May–October, circles) data are plotted separately. The intercepts of orthogonal distance regression lines (using the algorithm "fitexy" of Press et al., 1992) are $-28.1 \pm 1.0°/_{oo}$ ($r^2 = 0.95$, $n = 42$) for winter, and $-23.0 \pm 0.6°/_{oo}$ ($r^2 = 0.95$, $n = 35$) for summer.

composition of $-28.1 \pm 1.0^{\circ}/_{oo}$, close to the value for the global average fossil fuel source of $-28.5^{\circ}/_{oo}$ (Andres et al., 1995). Biogenic sources and sinks are generally heavier. This result indicates that wintertime regional sources are dominated by fossil fuel combustion.

In summer a much heavier ($-23.0 \pm 0.6^{\circ}/_{oo}$) CO_2 source/sink is indicated by the isotope measurements, consistent with the increased contribution of biological processes. The isotopic signature of photosynthesis by C_3 and C_4 plants differs significantly (e.g., Farquhar and Lloyd, 1993); the fractionation by C_3 plants averages about $-18^{\circ}/_{oo}$ (Tans et al., 1993), while fractionation by corn plants (C_4) grown at Clayton, NC (100 km NW of our site), in 1984 was around $-3.3^{\circ}/_{oo}$ (Marino and McElroy, 1991). If we assume that the measured summertime isotopic signature reflects only the processes of C_3 and C_4 photosynthesis, and decomposition of C_3 and C_4 plant material, acting on an atmospheric composition of $-7.8^{\circ}/_{oo}$ (M. Trolier, personal communication, 1994), then

$$f\varepsilon_4 + (1-f)\,\varepsilon_3 = -23.0^{\circ}/_{oo},$$

where ε_4 ($= -3.3^{\circ}/_{oo} - 7.8^{\circ}/_{oo}$) and ε_3 ($= -18.0^{\circ}/_{oo} - 7.8^{\circ}/_{oo}$) are the isotopic signatures for C_4 and C_3 photosynthesis, respectively, and f is the fraction of regional gross photosynthesis carried out by C_4 plants. Solving for f, we calculate that the contribution of C_4 plants to the isotope signal is about 19%; that is, gross photosynthesis by C_4 plants is about 19% of the total regional photosynthesis. A 10% contribution from fossil fuel combustion to the gross CO_2 surface source increases the calculated contribution by C_4 plants to around 23%, since the isotopically light fossil fuel carbon must be offset by additional heavy carbon. Here we have neglected the potential influence of CO_2 exchange with the ocean, which has a heavy isotope signature, and so would tend to reduce the computed contribution by C_4 plants. This analysis indicates that photosynthesis and respiration by C_3 plants is dominant in this region. The dominance of C_3 plants is probably not surprising, since most plants are C_3, but the data indicate that contribution to regional photosynthesis by corn, which is the dominant crop species and is C_4, is relatively minor. The other major crops (soybeans, tobacco and wheat) are C_3 species.

3.5. *Carbon monoxide and methane*

Carbon monoxide (CO) is a product of incomplete combustion of organic material (fossil fuel and biomass), and is also formed in the atmosphere from the photooxidation of methane (CH_4) and other hydrocarbons. Carbon monoxide is removed from the troposphere mainly by reaction with the hydroxyl radical, and the lifetime of CO in the troposphere at the latitude of the tower ranges from around 1 month in summer (when hydroxyl is most abundant) to greater than 12 months in winter (Novelli et al., 1992).

The relationship between CO and CO_2 in flask samples taken weekly from the 496 m level are shown in Fig. 8a. A strong linear relationship exists between CO and CO_2 at the tower in winter (November–March, slope $= 12.7 \pm 0.9$ ppb CO/ppm CO_2, $r^2 = 0.92$, $n = 31$, with 2 outliers removed based on examination of the residuals). The photochemical sources and sinks of CO, and the biogenic sources and sinks of CO_2, are slow in winter and the relationship in Fig. 8a likely reflects a combustion source for both species. The slope of the relationship is about 60% of that expected from CO and CO_2 emissions inventories from fossil fuel combustion in the US (J. Logan, personal communication, 1993; Bakwin et al., 1994), probably because a modest source of CO_2 from soil respiration continues in winter. Our results indicate that the wintertime respiration source of CO_2 is roughly two-thirds as large as the regional industrial source, that is about 0.2 kgC ha^{-1} h^{-1} (see above). In summer biogenic sources and sinks of CO_2 dominate fossil fuel sources, and we find no discernible relationship between CO and CO_2.

We also observe a significant linear relationship between CO and CH_4 in all seasons (Fig. 8b). The slope for wintertime data only is indistinguishable from the slope for all of the data, but the correlation is somewhat better in winter ($r^2 = 0.80$ for winter, $r^2 = 0.58$ for all data). This result probably reflects co-located industrial sources for CO and CH_4 (e.g., population centers). Apparently, throughout the year regional biogenic sources and sinks for CH_4 are small relative to urban-industrial sources.

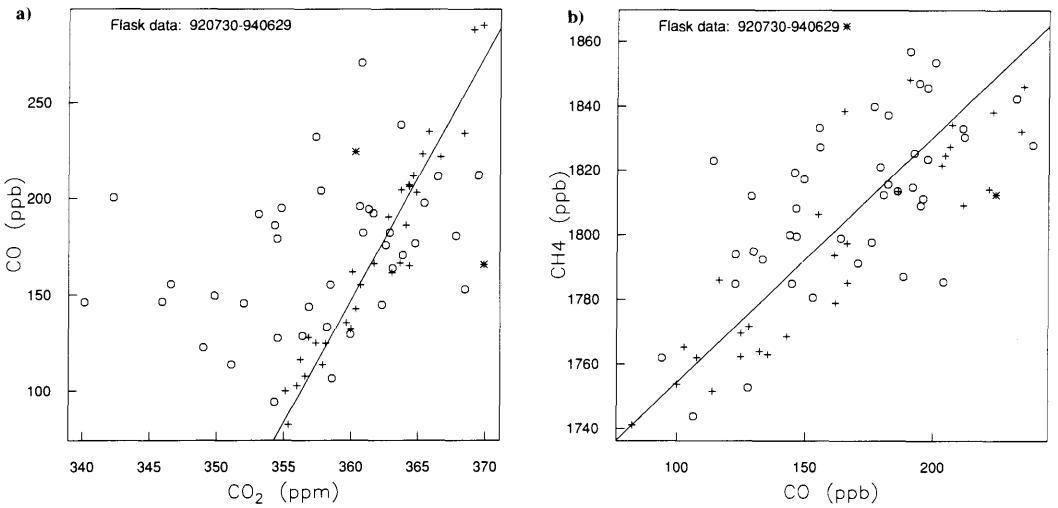

Fig. 8. (a) The relationship between CO and CO_2 in flask samples taken weekly from the 496 m level on the tower. Winter (November–February, plusses) and non-winter (circles) data are plotted separately, and the regression line (slope = 12.7 ± 0.9 ppb/ppm, $r^2 = 0.92$, $n = 31$) is an orthogonal distance regression fit to the wintertime data only, with 2 outliers (stars) excluded on the basis of examination of the residuals. (b) The relationship between CH_4 and CO in flask samples. The orthogonal distance regression line is fit to all of the data, and the slope is 0.76 ± 0.10 ppb/ppb ($r^2 = 0.58$, $n = 71$).

4. Conclusions

We present measurements of CO_2 mixing ratio at three altitudes up to 496 m above the surface on a commercial television transmitter tower in eastern North Carolina for a period of two years. The data show strong diurnal and seasonal variations, and large vertical gradients. The diurnal cycles are modulated by surface uptake and release by vegetation and soils, emissions from fossil fuel combustion, and by the diurnal development of the planetary boundary layer. Gradients of 1–2 ppm between 496 m and 51 m are typically observed during summertime afternoons, due to vigorous photosynthetic uptake. With increasing altitude the magnitude of the diurnal cycle is damped, and daily average mixing ratios decrease, caused by coincident changes in the sign and magnitude of the surface flux, and changes in vertical stability of the boundary layer over the course of the day. Measurements at 496 m give an approximate measure (within a few tenths of a ppm) of the afternoon CBL mean mixing ratio. Vertical gradients between 51 m and 496 m are typically close to zero, and monthly mean mixing ratios increase slowly between November and April, indicating that biological activity is minimal during this period.

The amplitude of the seasonal cycle of CO_2 is larger at the tower site than at the CMDL "background" sites which are at nearly the same latitude. This results from the proximity of the tower site to terrestrial sources and sinks, which mainly drive the seasonal cycle in the Northern Hemisphere (Fung et al., 1987). The comparison of the continental tower data with data from "background" sites (e.g., Fig. 6) should provide a strong constraint for regional and global models of terrestrial CO_2 fluxes.

Comparison of CO and CO_2 in weekly flask samples indicates that during winter biogenic CO_2 emissions are roughly two-thirds as large as emissions from fossil fuel combustion. The regional fossil fuel source, estimated at about 0.3 kgC $ha^{-1}\,h^{-1}$ for North Carolina, is sufficient to explain the occasional large build-up of CO_2 near the surface during winter inversion events, but biogenic sources dominate the nightly increase of CO_2 near the ground in summer.

Stable carbon isotope data ($\delta^{13}C$) from the flask

samples support the conclusion that fossil fuel sources are the dominant cause of CO_2 variations in winter. Summertime (May–October) isotope data indicate that photosynthesis by C_3 plants (e.g., trees, soybeans, tobacco and wheat) is substantially more important than by C_4 plants (e.g., corn). The regional landscape is a patchwork of agricultural fields and forest stands.

The data show an increase in CO_2 of about 2 ppm between the end of 1992 and the end of 1993, substantially larger than at the CMDL "background" sites in the Northern Hemisphere. This result could indicate a role for continental areas in modulating anomalies in the CO_2 growth rate, such as was observed during 1992 (Conway et al., 1994). Alternatively, interannual changes in mean atmospheric circulation or vertical mixing intensity could have influenced the measurements.

In this paper we have summarized results from the first two years of an on-going project. In future we expect to observe inter-annual variations of the seasonal cycle, and changes in the CO_2 mixing ratios relative to background sites, such as Bermuda. These changes should reflect variations in the net exchange of CO_2 with the regional terrestrial biosphere, but may also occur because of changes in atmospheric circulation patterns. Full understanding of the observed patterns will require integration of the tower data with the global "background" monitoring data within a global circulation model that includes a realistic representation of terrestrial biology and boundary layer dynamics (Denning, 1994). Recently we began measurements of CO_2 on a 450 m tall tower in northern Wisconsin (45.95° N). Comparison of boundary layer mixing ratios at these two sites should improve our understanding of atmosphere/surface exchange of CO_2 on the continental-scale.

5. Acknowledgements

We thank American Family Broadcasting for the very generous donation of space on the commercial transmitter tower and in the transmitter building, and Mr. A. Manning, chief engineer of WITN-TV, for invaluable assistance and advice. We are very grateful to CMDL staff for analysis of the flask samples and preparation and calibration of the CO_2 standards. This work was supported by the Atmospheric Chemistry Project of the Climate and Global Change Program of the National Oceanic and Atmospheric Administration and by the Environmental Protection Agency.

REFERENCES

Andres, R. J., Marland, G., Boden, T. and Bischoff, S. 1995. Carbon dioxide emissions from fossil fuel combustion and cement manufacture 1751–1991 and an estimate of their isotopic composition and latitudinal distribution. In: *The carbon cycle*, Proceedings of the Global Change Institute, Snowmass, Colorado, 19–30 July, 1993 (ed. T. Wigley, and D. Schimel). Cambridge University Press. In press.

Bakwin, P. S., Tans, P. P. and Novelli, P. C. 1994. Carbon monoxide budget in the Northern Hemisphere. *Geophys. Res. Lett.* **21**, 433–436.

Baldocchi, D. D., Verma, S. B. and Anderson, D. E. 1987. Canopy photosynthesis and water-use efficiency in a deciduous forest. *J. Appl. Ecol.* **24**, 251–260.

Ciais, P., Tans, P. P., White, J. W. C., Trolier, M., Francey, R. J., Berry, J. A., Randall, D. R., Sellers, P. J., Collatz, J. G. and Schimel, D. S. 1995. Partitioning of ocean and land uptake of CO_2 as inferred by $\delta^{13}C$ measurements from the NOAA/CMDL global air sampling network. *J. Geophys. Res.* **100**, 5051–5070.

Climate Analysis Center. 1994. *Climate diagnostics bulletin:* July 1994, (ed. V. Kousky). US Department of Commerce, Camp Springs, Maryland.

Conway, T. J., Tans, P., Waterman, L. S., Thoning, K. W., Masarie, K. A. and Gammon, R. H. 1988. Atmospheric carbon dioxide measurements in the remote global troposphere, 1981–1984. *Tellus* **40B**, 81–115.

Conway, T. J., Tans, P. P., Waterman, L. S., Thoning, K. W., Kitzis, D. R., Masarie, K. A. and Zhang, N. 1994. Evidence for interannual variability of the carbon cycle from the National Oceanic and Atmospheric Administration/Climate Monitoring and Diagnostics Laboratory global air sampling network. *J. Geophys. Res.* **99**, 22831–22856.

Davis, K. J. 1992. *Surface fluxes of trace gases derived from convective-layer profiles.* Ph.D. dissertation, University of Colorado, Boulder, Colorado, 281 pp.

Denning, A. S. 1994. *Investigations of the transport, sources, and sinks of atmospheric CO_2 using a general circulation model.* Ph.D. dissertation, Colorado State University, Fort Collins, Colorado, 335 pp.

Farquhar, G. D. and Lloyd, J. 1993. Carbon and oxygen isotope effects in the exchange of carbon dioxide between terrestrial plants and the atmosphere. In: *Stable isotopes and plant carbon-water relationships* (eds. J. R. Ehleringer, A. E. Hall and G. D. Farquhar). Academic Press, San Diego.

Fung, I. Y., Tucker, C. J. and Prentice, K. C. 1987. Application of advanced very high resolution radiometer vegetation index to study atmosphere-biosphere exchange of CO_2. *J. Geophys. Res.* **92**, 2999–3015.

Karnowski, E. H., Newman, J. B., Dunn, J. and Meadows, J. A. 1974. *Soil survey of Pitt County, North Carolina.* United States Department of Agriculture, Soil Conservation Service, Washington, DC, 73 pp.

Keeling, C. D. 1961. The concentrations and isotopic abundances of carbon dioxide in rural and marine air. *Geochim. Cosmochim. Acta* **24**, 277–298.

Keeling, C. D., Bacastow, R. B., Carter, A. F., Piper, S. C., Whorf, T. P., Heimann, M., Mook, W. G. and Roeloffzen, H. 1989. A three-dimensional model of atmospheric CO_2 transport based on observed winds (1). Analysis of observational data. In: Aspects of Climate Variability in the Pacific and Western Americas. *Geophys. Monogr. Ser.* **55** (ed. D. H. Peterson). Washington, DC, 165–236.

Marino, B. D. and McElroy, M. B. 1991. Isotopic composition of atmospheric CO_2 inferred from carbon in C_4 plant cellulose. *Nature* **349**, 127–131.

Marland, G., Andres, R. J. and Boden, T. A. 1994. Global, regional and national CO_2 emissions. In: *Trends'93: A compendium of data on global change* (eds. T. A. Boden, D. P. Kaiser, R. J. Sepanski and F. W. Stoss). ORNL/CDIAC-65. Carbon Dioxide Information and Analysis Center, Oak Ridge National Laboratory, Oak Ridge, Tennessee, 505–584.

Moeng, C.-H. and Wyngaard, J. C. 1984. Statistics of conservative scalars in the convective boundary layer. *J. Atmos. Sci.* **41**, 3161–3169.

Moeng, C.-H. and Wyngaard, J. C. 1989. Evaluation of turbulent transport and dissipation closures in second-order modeling. *J. Atmos. Sci.* **46**, 2311–2330.

Novelli, P. C., Steele, L. P. and Tans, P. P. 1992. Mixing ratios of carbon monoxide in the troposphere. *J. Geophys. Res.* **97**, 20731–20750.

Press, W. H., Teukolsky, S. A., Vetterling, W. T. and Flannery, B. P. 1992. *Numerical recipes in C*, 2nd edition. Cambridge University Press, Cambridge.

Sheffield, R. M. and Knight, H. A. 1986. *North Carolina's forests.* Southeast Forest Experiment Station Resource Bulletin SE-88. US Department of Agriculture, Asheville, NC, 97 pp.

Steele, L. P., Fraser, P. J., Rasmussen, R. A., Khalil, M. A. K., Conway, T. J., Crawford, A. J., Gammon, R. H., Masarie, K. A. and Thoning, K. W. 1987. The global distribution of methane in the troposphere. *J. Atmos. Chem.* **5**, 125–171.

Stull, R. B. 1988. *An introduction to boundary layer meteorology.* Kluwer Academic Publishers, Dordrecht, 666 pp.

Tans, P. P. 1991. An observational strategy for assessing the role of terrestrial ecosystems in the global carbon cycle: scaling down to regional levels. In: *Scaling processes between leaf and landscape levels* (ed. J. Ehleringer and C. Field). Academic Press, San Diego.

Tans, P. P., Fung, I. Y. and Takahashi, T. 1990. Observational constraints on the global atmospheric CO_2 budget. *Science* **247**, 1431–1438.

Tans, P. P., Berry, J. A. and Keeling, R. F. 1993. Oceanic $^{13}C/^{12}C$ observations: a new window on oceanic CO_2 uptake. *Global Biogeochem. Cycles* **7**, 353–368.

Thoning, K. W., Tans, P. P., Conway, T. J. and Waterman, L. S. 1987. *NOAA/GMCC calibrations of CO_2-in-air reference gases: 1979–1985.* NOAA Tech. Memo., ERL ARL-150.

Thoning, K. W., Tans, P. P. and Komhyr, W. D. 1989. Atmospheric carbon dioxide at Mauna Loa observatory, 2. Analysis of the NOAA GMCC data, 1974–1985. *J. Geophys. Res.* **94**, 8549–8565.

US Department of Commerce. 1989. *Census of Agriculture 1987, North Carolina, Part 33.* US Government Printing Office, Washington, DC, 489 pp.

Wofsy, S. C., Goulden, M. L., Munger, J. W., Fan, S.-M., Bakwin, P. S., Daube, B. C., Bassow, S. L. and Bazzaz, F. A. 1993. Net exchange of CO_2 in a mid-latitude forest. *Science* **260**, 1314–1317.

Wyngaard, J. C. and Brost, R. A. 1984. Top-down and bottom-up diffusion of a scalar in the convective boundary layer. *J. Atmos. Sci.* **41**, 102–112.